

A&A manuscript no.
(will be inserted by hand later)

Your thesaurus codes are:
02 (11.03.4 Coma cluster; 04.03.1; 11.03.1; 11.04.1; 11.12.2)

ASTRONOMY
AND
ASTROPHYSICS

Deep probing of the Coma cluster. ^{*}

C. Adami¹, R.C. Nichol², A. Mazure¹, F. Durret^{3,4}, B. Holden⁵, C. Lobo^{3,6}

¹ IGRAP, Laboratoire d'Astronomie Spatiale, CNRS, Traverse du Siphon, Les Trois Lucs, F-13012 Marseille, France

² Department of Physics, Carnegie Mellon University, 5000 Forbes Avenue, Pittsburgh, PA 15213, USA

³ Institut d'Astrophysique, CNRS, Université Pierre et Marie Curie, 98bis Bd Arago, F-75014 Paris, France

⁴ DAEC, Observatoire de Paris, Université Paris VII, CNRS (UA 173), F-92195 Meudon Cedex, France

⁵ Department of Astronomy and Astrophysics, University of Chicago, 5640 S. Ellis Avenue, Chicago, Illinois 60637, USA

⁶ Osservatorio Astronomico di Brera, via Brera 28, I-20121 Milano, Italy

Received date; accepted date

Abstract. As a continuation of our study of the faint galaxy luminosity function in the Coma cluster of galaxies, we report here on the first spectroscopic observations of very faint galaxies ($R \leq 21.5$) in the direction of the core of this cluster. Out of these 34 galaxies, only one may have a redshift consistent with Coma, all others are background objects. The predicted number of Coma galaxies is 6.7 ± 6.0 , according to Bernstein et al. (1995, B95). If we add the 17 galaxies observed by Secker (1997), we end up with 5 galaxies belonging to Coma, while the expected number is 16.0 ± 11.0 according to B95. Notice that these two independent surveys lead to the same results. Although the observations and predicted values agree within the error, such results raise into question the validity of statistical subtraction of background objects commonly used to derive cluster luminosity functions (e.g. B95). More spectroscopic observations in this cluster and others are therefore urgently needed.

As a by-product, we report on the discovery of a physical structure at a redshift $z \simeq 0.5$.

Key words: Cluster: individual: Coma cluster- Clusters: general - Galaxies: Catalogs - Galaxies: distances and redshifts- Galaxies: luminosity function, mass function.

1. Introduction

The Coma cluster of galaxies is one of the most intensively studied clusters in the sky. Its high richness and low redshift have led it to become the archetypal target for both observational and theoretical cluster studies. However, one aspect of Coma that has not yet been fully investigated is the distribution and dynamics of faint cluster galaxies.

Send offprint requests to: C. Adami, adami@astrsp-mrs.fr

^{*} Based on observations collected at the Canada France Hawaii telescope, operated by the National Research Council

Indeed, we do not fully know what contribution galaxies fainter than the photographic plate limit (cf. the photometry by Godwin et al. 1983) make to the overall light (and mass) of Coma, and whether this contribution can significantly increase the known baryonic mass in the cluster. Furthermore, the exact shape of the Coma luminosity function (Bernstein et al. 1995, hereafter B95, Biviano et al. 1995, Lobo et al. 1997, Trentham 1997) remains in doubt, with suggestions varying from a single atypical Schechter function with a steep faint end slope to a Gaussian at bright magnitudes and a power-law at the faint end. This confusion comes from the reliance on a 2D statistical correction to subtract the background contribution. Most papers analyzing cluster luminosity functions, especially in distant clusters, use this method (see e.g. Driver et al. 1994, De Propriis et al. 1995), but such a procedure could induce severe correlated errors and biases. Although the large error bars on these predictions do not totally prohibit a conclusive statement on potential errors in the 2D statistical background subtraction, it is crucial to check carefully this method. Coma is an excellent first candidate for this purpose. In the present paper, we assume $H_0 = 100 \text{ km s}^{-1} \text{ Mpc}^{-1}$ and $q_0 = 0$.

2. The sample

2.1. Photometry

The photometric sample on which our study is based is one of the deepest images presently available of the Coma cluster core taken by B95. The data are complete to the CCD magnitude $R=25$ which is far beyond the photographic plate limit of Godwin et al. (1983). The size of the field is $7.5 \times 7.5 \text{ arcmin}^2$ and is centered on coordinates $12^{\text{h}} 57^{\text{m}} 17^{\text{s}}$; $28^\circ 09' 35''$ (equinox 1950, as hereafter). This area corresponds to the core of the Coma cluster near NGC 4874 and NGC 4889. For the spectroscopic observations, we have restricted the investigation

eter $0.85 < \mathfrak{R} < 2.2$ (see B95, Fig. 3); there is a very low probability to have stars or globular clusters in the sample according to the B95 criteria. Note that in this range of magnitudes, the Coma cluster luminosity function may rise significantly towards faint magnitudes (e.g. Lobo et al. 1997), and the background-to-cluster galaxy ratio is already high ($\simeq 3.4$: ratio based on Table 2 of B95). Going fainter would only result in more background galaxies. For 99 of these 105 galaxies, a b_j magnitude is also available. These b_j magnitudes were observed at the same time as the R data but are not the same signal-to-noise.

Additionally, we have checked the magnitudes of B95 by using the photographic $b_{26.5}$ and $r_{24.75}$ faintest magnitudes of Godwin et al. (1983). We have found 12 common galaxies in the two samples. Even if the two systems are not directly comparable, we find well constrained relations, which support the B95 photometry:

$$b_j = (0.95 \pm 0.09) b_{26.5} + (0.54 \pm 0.22)$$

and

$$R = (0.80 \pm 0.10) r_{24.75} + (-1.12 \pm 0.19)$$

2.2. Spectroscopy

We have observed spectroscopically some of the targets using the 3.6m CFHT with the MOS spectrograph during three nights in March 1997. Because of the bad weather, only half a night was available, during which we have obtained spectra for 43 objects out of the 105 selected from the B95 total sample. Two exposures of 1 hour have been used for each mask. The first mask was exposed with many intermittent and diffuse clouds and the spectra of one of the two exposures were cut by a wrongly placed R filter. We preferentially chose B95 objects, but we also put slits on randomly selected objects with a galaxy appearance to optimize the number of slits per mask.

We have corrected for the well known geometrical distortion of MOS with the Geotran task in IRAF. The data reduction itself was made with the ESO MIDAS classical reduction procedure package.

The redshifts were deduced by fitting gaussian profiles on well identified lines. If there were emission and absorption lines in the same spectrum, we selected emission lines to deduce the redshift. We got 30 spectra (Table 1) with more than two emission lines for the emission line galaxies (ELG hereafter), or H&K absorption lines and the 4000Å break for the galaxies with only absorption lines (ALG hereafter).

For four other spectra, we had only one line available. We could deduce a redshift for two of them by using the shape of this line or the absence of other lines (Table 1). For the last two, we have three possibilities. The first redshift could be 1.3284 ± 0.0017 ([OII]), 0.7854 ± 0.0013 (H β) or 0.3224 ± 0.0010 (H α). The second one could be 1.3108 ± 0.0022 ([OII]), 0.7719 ± 0.0017 (H β) or $0.3124 \pm$

[OIII] λ 4959 and [OIII] λ 5007 emission lines. We therefore use the respective mean wavelengths of these two sets of lines to determine redshifts.

To test the reliability of our data, we also used the cross-correlation task RVSAO/XCSAO in IRAF to measure radial velocities. We selected the five best sky subtracted spectra which exhibit absorption lines and adopted as templates two reference spectra: M31 and a synthetic spectrum of stars, and used 50 iterations. The results are consistent with the redshifts obtained by line identifications (see Table 1). For the best correlation coefficient cR, the mean difference is only 2% between the line estimated redshift and the template estimated redshift. The only exception is for the galaxy at $z=0.6773$, with a difference of 9%. But in this case, cR is very low for both templates and the result is not reliable.

The mean final success rate for extracting redshift measurements from the spectra was 70% for the two masks, and 76% for the mask “2” observed in good conditions (for the B95 targets). As a measure of the quality of the B95 galaxy/star separation, we note here that almost no globular clusters or stars were accidentally observed.

Finally, we end up with 34 redshifts (secure:30 ; secure with one line:2 ; with several possibilities: 2; see Table 1 and Fig. 1). Among these 34 galaxies, 29 have a magnitude (from B95) and five are supplementary galaxies. Fig. 1 shows a typical spectrum at $z=0.5034$ with the [OII] (5604Å), and H&K (around 6000Å) lines clearly visible. We have 24 ELG and 10 ALG. The error on the redshift is taken as the tenth of the FWHM of the fitted gaussian for a given line. For the only galaxy which clearly shows emission and absorption lines, the two estimations are consistent: 0.5034 ± 0.0016 and 0.5071 ± 0.0018 .

We added to our sample of 29 galaxies with a magnitude the 17 galaxies in the range of R magnitude [15.5;20.5] and with a (b_j -R) colour in the range [0.7;1.9] spectroscopically observed by Secker et al. (1997, hereafter S97). Interestingly, these two independent surveys lead to the same results (see below). Our total sample with redshifts is therefore 46 galaxies.

3. Analysis

3.1. The redshift distribution observed along the Coma line of sight

The 29 successfully observed galaxies from the B95 sample (i.e. with an available magnitude) are a random subsample of the global sample of 105 galaxies (Fig. 2), as indicated by the comparable magnitude distributions of the sample and subsample; a Kolmogorov-Smirnov test indeed confirms that the probability for these two distributions to be different is only 0.1%. Hence, there is no obvious bias in the object selection. The 32 secure redshifts (30 with more than 2 lines and 2 with the shape of the line) are

Table 1. Table of the secure redshifts with more than 2 lines (ALG or ELG) or secure with the shape of the line: galaxy location in arcmin with respect to the center 12h 57m 17s; 28° 09' 35", R and b_j magnitudes, absolute magnitude M_R , line used to determine the redshift and other available lines. The velocities obtained with a template analysis are also given for the two templates used with their Tonry & Davis (1979) correlation coefficient in parentheses. The galaxies of the distant cluster are marked with an asterisk.

Redshift	A/ELG	(x,y) (arcmin)	R	b_j -R	M_R	Line	Other lines	Redshift M31	Redshift stars
0.3233 ± 0.0005	ELG	5.02,0.87	/	/	/	H β	[OIII]		
0.8765 ± 0.0014	ELG	4.69;-2.96	/	/	/	[OII]	[OIII]		
0.5791 ± 0.0010	ELG	4.61;0.01	/	/	/	[OII]	[OIII]		
0.8765 ± 0.0014	ELG	4.15;1.35	/	/	/	[OII]	[OIII]		
0.8242 ± 0.0010	ALG	3.70;-0.80	/	/	/	H&K			
0.8294 ± 0.0007	ALG	3.22;-2.69	20.55	1.06	-25.23	H&K		0.6699 (2.2)	0.8540 (2.4)
0.6773 ± 0.0010	ELG	2.95;1.33	20.78	1.97	-21.50	[OII]	[OIII], H&K?	0.4909 (1.1)	0.7440 (1.3)
0.3069 ± 0.0009	ELG	2.45;-2.32	19.85	1.31	-20.30	[OII]	[OIII], H α		
0.2405 ± 0.0008	ELG	1.79;2.80	21.28	0.94	-18.27	H α	[OIII]		
0.7696 ± 0.0008	ELG	1.35;-0.55	20.97	1.25	-21.68	[OII]	H β		
0.2593 ± 0.0008	ELG	1.04;0.07	21.11	1.29	-18.64	H α	[OIII]		
0.2512 ± 0.0005	ELG	1.37;1.92	20.42	1.36	-19.24	H α	[OII], H β		
0.5678 ± 0.0019	ALG	0.20;-0.92	20.45	2.44	-21.32	H&K			
0.4496 ± 0.0011	ELG	1.26;-0.75	21.20	1.10	-19.94	H β	[OIII]		
0.6092 ± 0.0009	ELG	1.08;-0.22	21.26	/	-20.71	[OII]	[OIII]		
0.6586 ± 0.0007	ELG	0.83;-1.30	20.98	0.89	-21.21	[OII]	[OIII]		
0.2415 ± 0.0009	ELG	-0.78;2.19	20.16	1.51	-19.40	H α	[OIII]		
0.4560 ± 0.0009	ELG	0.62;0.15	21.07	1.34	-20.11	[OII]	[OIII]		
*0.5108 ± 0.0006	ALG	-2.37;1.11	20.25	2.33	-21.23	H&K	G	0.5136 (2.4)	0.5135 (1.7)
0.4440 ± 0.0008	ELG	-0.41;2.93	21.02	2.01	-20.08	H β	[OIII], H α ?		
*0.5209 ± 0.0012	ALG	-2.61;2.64	20.43	2.28	-22.93	H&K	H α ?		
0.2644 ± 0.0007	ALG	-0.54;-0.96	19.30	1.59	-20.48	H&K			
*0.5000 ± 0.0100	ALG	-2.77;1.41	19.77	1.78	-23.40	4000 A	H&K		
0.4266 ± 0.0003	ELG	-0.93;2.03	20.97	1.11	-20.03	[OII]	H β , [OIII]		
*0.5188 ± 0.0020	ALG	-3.03;0.37	19.48	1.69	-23.86	H&K	[OII]?		
0.1760 ± 0.0006	ELG	-1.11;2.63	19.32	0.96	-19.48	[OIII]	H α		
0.3290 ± 0.0008	ELG	-1.72;-1.26	19.65	1.45	-20.68	H α	H β		
0.6014 ± 0.0006	ELG	-2.15;-1.56	20.30	1.03	-21.63	H β	[OIII]		
*0.5034 ± 0.0016	A/ELG	-2.81;0.58	20.45	2.23	-20.99	[OII]	H α , H&K	0.5194 (4.2)	0.5187 (4.5)
*0.5104 ± 0.0025	ALG	-3.14;1.22	18.99	2.12	-22.49	H&K		0.5188 (5.0)	0.5163 (3.7)
0.0227 ± 0.0006	ELG	1.66;1.02	21.30	1.72	-12.89	[OIII]	Shape of the line		
0.7213 ± 0.0005	ELG	-1.95;2.25	20.83	1.04	-21.63	[OIII]	Shape of the line		

one galaxy in the Coma cluster at $z=0.023$ and a little density peak at $z \simeq 0.5$. B95 predicted for the [19.0;21.5] R magnitude range and for a total of 29 galaxies (these 29 are with a magnitude) that only 6.7 ± 6 galaxies should be in Coma (see Table 2 in B95). This is consistent at 1σ with only 1 galaxy in Coma (we do not take into account the five supplementary observed galaxies because we do not know their magnitudes), but the error bar is very large. Note that the error on the background counts is calculated with robust estimators (see B95 for details).

The B95 counts (as well as the S97 ones) predict

in the cluster, a result comparable to that obtained with our sample.

Before merging both samples, we checked for possible redundant galaxies. The fields of B95 and S97 cover the same area, but the magnitude distributions are different. Only 14 out of our 29 spectroscopically observed galaxies (with an available magnitude) are in the range R [15.5;20.5]. Out of these 14, only 9 have a color in the range [0.7;1.9]. Moreover, a large fraction of the redshifts of S97 which are not Coma members are at $z \simeq 0.2$. Among our 9 remaining galaxies, only 4 are at $z \leq 0.3$. We therefore

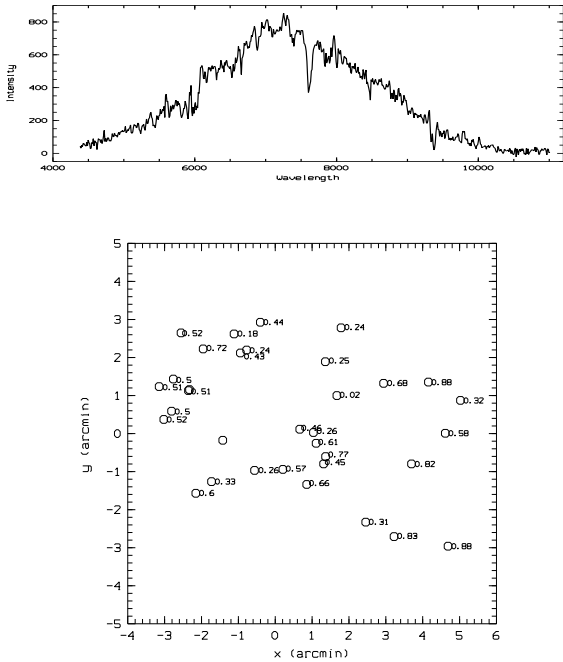


Fig. 1. Top: typical spectrum with the [OII] and H&K lines clearly visible (not corrected for the instrument response function). Bottom: 2D map of the successfully observed galaxies with the corresponding redshift. The two unlabelled circles are the two galaxies with many solutions for the redshift (second unlabelled circle nearly superposed with the redshift 0.51: upper left side of the figure).

Consequently, for the 46 redshifts in this paper in the direction of Coma (obtained by putting together our data and those of S97), only 5 are in Coma. B95 would predict 16 ± 11 in the corresponding range of magnitudes. Once again, these numbers are consistent at only 1σ , but with a very large error bar. This raises into question the faint end of the cluster luminosity function derived by B95.

If we try to apply the photometric criteria based on the color-magnitude relation, or *CMR* (e.g. Mazure et al. 1988), to define the cluster membership up to the magnitude limit of B95, we obtain a puzzling result. We plot in Fig. 4 all the galaxies in the range R [17;25] with a color available. We observe a concentration of objects in the color range [0.85;1.30], consistent with the value $b_j - R = 1.28$ given in Frei & Gunn (1994) for elliptical galaxies at $z=0.0$. According to the color criterion, we expect that 50% of the galaxies with magnitudes between $R=18.98$ and 21.5 should be in Coma. However, the number deduced from the spectroscopic observations is very different, and moreover the $b_j - R$ colour of the sin-

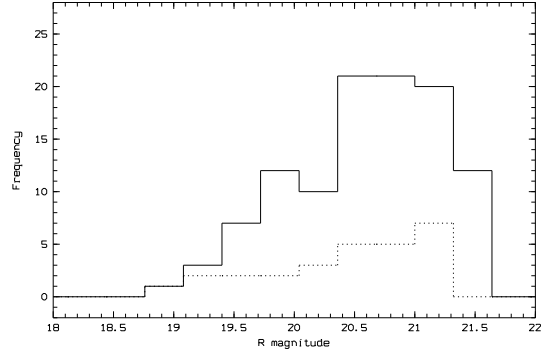


Fig. 2. Histogram of the 105 selected galaxy magnitudes in the $18.98 \leq m_R \leq 21.5$ range (solid line) and of the 27 successfully observed spectroscopically, which have only one possible redshift (dashed line) and with an available magnitude.

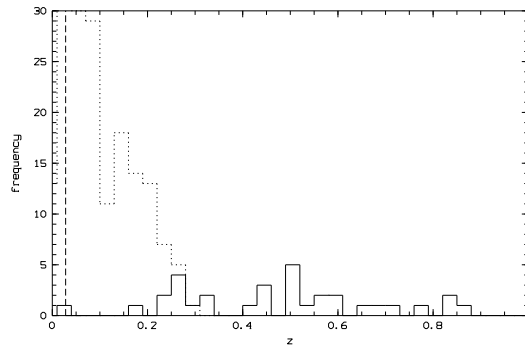


Fig. 3. Histogram of the 32 redshifts (solid histogram) and of the already available redshifts (dashed line) on the Coma line of sight. The vertical long-dashed line symbolizes the maximum distance for the Coma cluster assuming $z_{Coma} = 0.0232$ and $\sigma_{v,Coma} = 1000 \text{ km s}^{-1}$.

must therefore use this criterion with caution. A possible explanation for this lack of faint Coma members in this particular region of the cluster could be their tidal disruption in the core of the cluster, as described by S97.

The existence of faint galaxies much redder than the red envelope of the *CMR* is important. This could be taken as an indicator of large metallicities for these dwarf galaxies, which are possible due to the confinement of these systems by the intra-cluster medium (see S97). We show in Fig. 5 the spectrum of this galaxy obtained by summing the two exposures, together with a zoom of the only available emission line from the first exposure with the best S/N ratio. Clearly, this line is not $H\beta$ because we do not see $H\alpha$ at 6700 \AA . The remaining choices are [OII] and [OIII]. The shape of this line is more consistent with

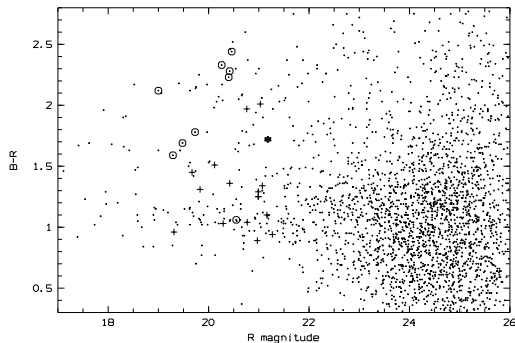


Fig. 4. (b_j -R, R) distribution of the galaxies between $R=17$ and 25 with secure redshift and color available. The galaxies observed spectroscopically are crossed, the ALG are circled and the only galaxy in Coma is the star.

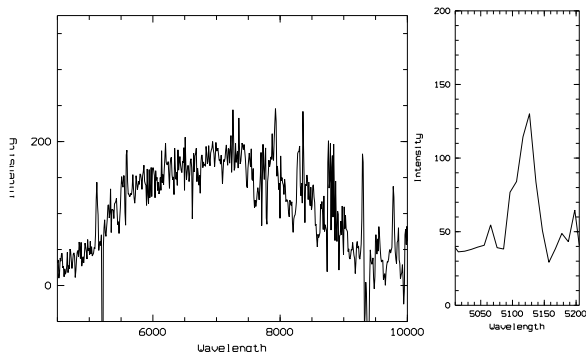


Fig. 5. Spectrum of the galaxy supposed to be in Coma. Left: overall spectrum; right: zoom of the only available emission line.

and with a b_j -R color equal to 1.72 (see Table 1). We have checked this color ourselves and confirm the value of 1.72. We note here that the absolute magnitude of the observed Coma galaxy is -12.89 , consistent with faint dwarf galaxy magnitudes (e.g. Patterson & Thuan 1996, Stein et al. 1997). However, this redshift obviously needs to be confirmed, and it is possible that this galaxy is also a background object (or a very faint star), in which case there would be NO galaxy in Coma out of the 34 objects that we observed.

We have a high percentage of ELG (70% of the sample), but this is not surprising, in view of the small number of galaxies in a dense environment observed along this line of sight. Although it is possible that we are underestimating the fraction of galaxies in Coma at these magnitudes, it is a well known fact that ELG occur more frequently in the field than in clusters (see Biviano et al. 1997 for complete references). Moreover, the percentage of 70%

3.2. A physical structure at $z \simeq 0.5$ beyond the Coma cluster

B95 reported the discovery of an optical subclump of galaxies (approximately at $\alpha = 12^{\text{h}} 57^{\text{m}} 14^{\text{s}}$; $\delta = 28^{\circ} 08' 30''$) in their deep image of Coma. We have sampled this subclump (see Fig. 1 and Table 1) with 6 redshifts. They all correspond to the peak at $z=0.5$ of Fig. 3 and the spatial extension is 360 kpc at $z=0.5107$ (mean redshift of the structure). If we assume a random distribution of 34 galaxies in the (x,y,z) space where z is in the $[0.17;0.88]$ range and (x,y) is a 7.5×7.5 arcmin square, the probability of having 6 galaxies clustered both in redshift and angularly is less than $2 \cdot 10^{-10}$.

Moreover, these 6 galaxies are ALG and represent 60% of all the ALG in the spectroscopic sample. If we keep only these 6 galaxies with H&K lines (and with a template velocity when available), their velocity dispersion is 660 km s^{-1} (calculated at $z=0$), which is consistent with a cluster of galaxies, but too high for a group of galaxies (e.g. Barton et al. 1996). Furthermore, this structure does not correspond to any of the Rose (1977), Hickson (1982) or Barton et al. (1996) groups. We note that four of these six galaxies have a b_j -R color equal to 2.25, only moderately inconsistent with the range of values calculated by Frei & Gunn (1994) for the elliptical galaxies between $z=0.4$ and 0.6: $[2.43;2.5]$. We may have observed the brightest members of a distant cluster at $z \simeq 0.5$ beyond Coma.

4. Conclusions

As presented above, 34 faint galaxy redshifts have been obtained in the direction of the Coma cluster core: 29 galaxies have magnitudes in the range $19 \leq R \leq 21.3$, and 5 do not have measured magnitudes. Out of these 34 galaxies, only one may have a redshift consistent with the Coma cluster, all the others being background objects. If we add the S97 results, we obtain a more representative sample of 46 redshifts along the Coma line of sight, out of which only 5 are in the cluster. Notice that these two independent surveys lead to the same results. Although the number of galaxies found to be in Coma is consistent at the 1σ level with the expected number of objects in Coma predicted by B95 (16 ± 11), such a result obviously raises into question the validity of the statistical subtraction of background objects. Tidal disruption can be proposed as an explanation of the apparent deficit of faint galaxies in this region of the core of the Coma cluster. Moreover, the presence of a distant cluster on the same line of sight probably increases the field counts. However, more spectroscopic observations of very faint galaxies are obviously needed; we are pursuing more data in this Coma field, but prefer to release the present data to encourage other observers to also obtain

Acknowledgements. We are indebted to Mel Ulmer and Gary Bernstein for making available all the deep Coma photometry from Bernstein et al. (1995) and for initially being involved in this project sometime ago. C.A. thanks V. Lebrun for his help during the data reduction and for helpful discussions. C.A. thanks the french GDR of Cosmology, CNRS, for financial support. B.H. acknowledges the Center for Astrophysical Research in Antarctica, NSF OPP 89-20223, for partial financial support. During this project, C.L. was fully supported by the BD/2772/93RM grant attributed by JNICT, Portugal. The authors also wish to thank the CFHT time allocation committee, the night staff and the referee for useful comments.

References

- Barton E., Geller M.J., Ramella M., Marzke R.O., da Costa L.N., 1996, AJ 112, 871
- Bernstein G.M., Nichol R.C., Tyson J.A., Ulmer M.P., Wittman D., 1995 AJ 110, 1507
- Biviano A., Durret F., Gerbal D. et al., 1995, A&A 297, 610
- Biviano A., Katgert P., Mazure A. et al., 1997, A&A 312, 84
- De Propris R., Pritchett C.J., Harris W.E., McClure R.D. 1995, ApJ 450, 534
- Driver S.P., Phillipps S., Davies J.I., Morgan I., Disney M.J. 1994, MNRAS 268, 393
- Frei Z., Gunn J.E., 1994, AJ 108, 1477
- Godwin J.G., Metcalfe N., Peach P.V., 1983, MNRAS 202, 113
- Hickson P., 1982, ApJ 255, 382
- Lobo C., Biviano A., Durret F. et al., 1997, A&A 317, 385
- Mazure A., Proust D., Mathez G., Mellier Y., 1988, A&AS 76, 339
- Patterson R.J., Thuan T.X., 1996, ApJSS 107, 103
- Rose J.A., 1977, ApJ 211, 311
- Secker J., Harris W.E., Cote P., Oke J.B., 1997, Proc. "A New Vision of an Old Cluster: Untangling Coma Berenices", Marseille June 1997, Eds. Mazure et al., astro-ph 9709053: S97
- Stein P., Jerjen H., Federspiel M., 1997, A&A 327, 952
- Tonry J., Davis M., 1979, AJ 84, 1511
- Trentham N. 1997, astro-ph 9708189
- Tresse L., Rola C., Hammer F. et al., 1996, MNRAS 281, 847